

Aerial image semantic segmentation based on 3D fits a small dataset of 1D

Shouket Abdulrahman Ahmed¹, Hazry Desa¹, Abadal-Salam T. Hussain^{1,2}

¹Centre of Excellence for Unmanned Aerial Systems (COEUAS), Universiti Malaysia Perlis, Jalan Kangar-Alor Setar, Kangar, Malaysia

²Department of Medical Instrumentation Engineering Techniques, Al-Kitab University, Altun Kupri, Iraq

Article Info

Article history:

Received Jul 1, 2022

Revised Mar 31, 2023

Accepted Apr 12, 2023

Keywords:

Aerial image

Dataset 3D modeling of 1D

Semantic segmentation

Unmanned aerial vehicle

ABSTRACT

Time restrictions and lack of precision demand that the initial technique be abandoned. Even though the remaining datasets had fewer identified classes than initially planned for the study, the labels were more accurate. Because of the need for additional data, a single network cannot categorize all the essential elements in a picture, including bodies of water, roads, trees, buildings, and crops. However, the final network gains some invariance in detecting these classes with environmental changes due to the different geographic positions of roads and buildings discovered in the final datasets, which could be valuable in future navigation research. At the moment, binary classifications of a single class are the only datasets that can be used for the semantic segmentation of aerial images. Even though some pictures have more than one classification, images of roads and buildings were only found in a significant number of samples. Then, the building datasets were pooled to produce a larger dataset and for the constructed models to gain some invariance on image location. Because of the massive disparity in sample size, road datasets needed to be integrated.

This is an open access article under the [CC BY-SA](#) license.



Corresponding Author:

Shouket Abdulrahman Ahmed

Centre of Excellence for Unmanned Aerial Systems (COEUAS), Universiti Malaysia Perlis

Jalan Kangar-Alor Setar, 01000 Kangar, Perlis, Malaysia

Email: shouketunimap@gmail.com

1. INTRODUCTION

There is currently a scarcity of aerial imaging data with pixel-level annotations for semantic segmentation. This is because labeling several types of objects in high-resolution images is a time-consuming process. This section will go over an initial method of manually hand-labeling data, the final datasets that were used, and the necessary preparations [1].

The Semantic Drone Dataset focuses on improving the safety of autonomous drone flying and landing processes by using semantic comprehension of urban settings. More than 20 buildings are depicted in the imagery, which was captured from a nadir (bird's eye) view at the height of 5 to 30 meters distant from the ground [2]–[4]. Images with a resolution of 6,000×4,000px were captured with a high-resolution camera (24Mpx) 5,6. The training set has 400 publicly available photographs, whereas the test set contains 200 private images. Objects in the image are listed as shown in Table 1 and Figure 1.

The lack of adequately annotated aerial images led to the creation of a new dataset as a first step. The Institute für Maschinelles Sehen and Darstellen, Graz, provided this new dataset, which consisted of randomly modified images. The algorithm that was utilized to obtain the data is described. 1,000 images were selected randomly from the flight test database using this approach. A Microsoft Surface tablet, together with an Image Labeler from MATLAB toolbox were used to label each of these images. The labeling was done in three classes which are buildings, roads, and clouds. Figure 2 shows an example of one of the many labeled images. In

Figure 2(a), a settlement is depicted, which was selected as a test case to evaluate the developed method. The settlement represents a specific area or location of interest where the method was applied. By examining Figure 2(a), we can observe the characteristics and features of the settlement, such as buildings, roads, and other structures. To provide a more comprehensive analysis, Figure 2(b) presents the processed street view derived from Figure 2(a). This processed image emphasizes the street-level perspective, highlighting the details and elements relevant to the assessment conducted using the developed method. By focusing on the street view, we can gain a clearer understanding of the specific attributes and conditions present within the settlement.

Table 1. List of objects in images

Objects name	Objects name	Objects name	Objects name
Unlabelled	Door	Bicycle	Rocks
Paved-area	Fence	Tree	Pool
Dirt	Fence-pole	Bald-tree	Vegetation
Grass	Person	Ar-marker	Roof
Gravel	Dog	Obstacle	Wall
Water	Car	Conflicting	Window



Figure 1. List of objects in images

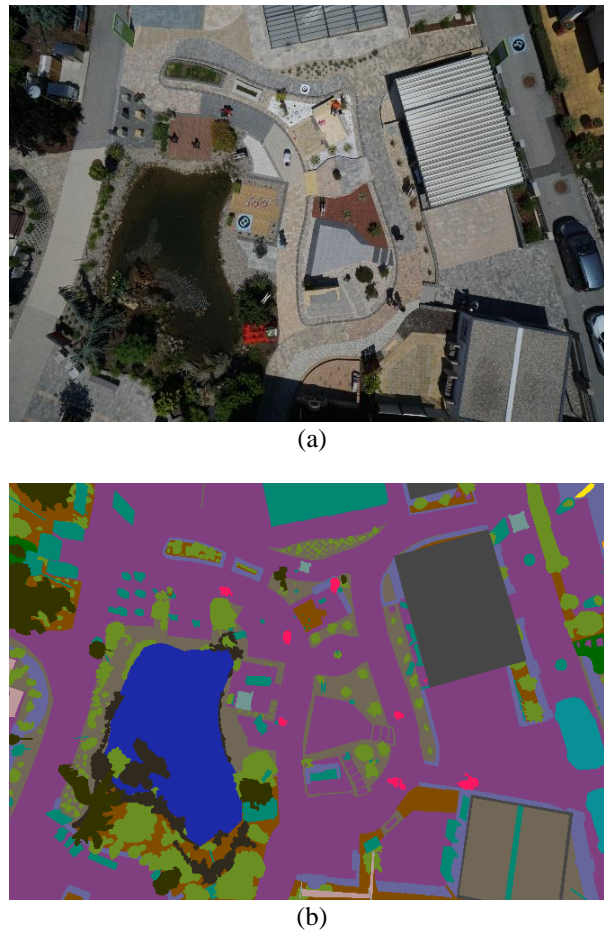


Figure 2. Sample of initial hand-label approach (a) image block and (b) streets labeled as lines in the images

2. METHOD

Explaining research chronological, including research design, research procedure (in the form of algorithms, Pseudocode or other), how to test and data acquisition [2]–[4]. The description of the course of research should be supported references, so the explanation can be accepted scientifically [5], [6]. Figures 1 and 2 and Table 1 are presented center, as shown and cited in the manuscript [2], [7]–[12]. The settlement curves produced at SG1 has been illustrated in Figure 2(a) and SG2 has been illustrated Figure 2(b).

2.1. Pre-processing

The existing computational limits restrict the integration of full-sized high-resolution imagery into a CNN; the training cannot be done efficiently due to computational issues (memory) [7]–[9]. This necessitates preprocessing the images into smaller enhanced patches that will be used to train and test the models 10. The final prediction model was developed by mask, the final test images are resized back from the patches 11. Normalization of the spatial resolutions was also done for it to be used in the final integrated buildings dataset. Being that this is a popular semantic segmentation resolution, coupled with the availability of computing resources, the input image crops were chosen to have a resolution of 224×224 pixels. Image data generators were built in each step in the epoch for use with Keras, yielding batches of 32 randomly enhanced 224×224 crops from the high-quality images. In this project, the utilized random augmentations include horizontal flips, rotations, and vertical flips. The "mirror" fill mode was employed, which takes the vacant areas of the image generated by rotation and mirrors it until such areas are filled. Being that aerial imagery is not usually homogeneous to one orientation, the model can rely on these augmentations to learn from diverse perspectives. This also creates artificially additional training data that can be learned by the model for pattern generalization.

2.2. Data pre-processing

The images were subjected to data augmentation before the training step [12]–[14]. The data augmentation was aimed at improving the dataset's size and performance, as well as the capacity to generalize

patterns. The pixel values were additionally normalized to make them between 0 and 1, with the goal of obtaining the loss-optimized value using gradient descent with fewer epochs. Data normalization enhances learning and generally improves the convergence speed. Image flipping can be done either vertically or horizontally or both. However, not all frameworks support vertical flips [15], [16]. A vertical flip is nothing but the rotation of an image by 180°, followed by its horizontal flipping. Horizontal flip is simply the horizontal reversing of all the columns and rows of an image pixel while the vertical flip is simply the vertical reversal of the entire columns and rows of an image pixel.

2.3. Cropping and image normalization

The select a piece of the original image at random. This part is then resized to the original image size. Random cropping is a frequent term for this technique. Image normalization is the important step for the training part because deep neural networks are all about writing a cost function and optimizing it so this will revolve around optimizer so to optimize the cost function in a smaller number of epochs its mandatory to do normalization or standardization but in case of images, normalization is the best approach [7]–[13] [14]–[19].

2.4. Gradient descent algorithm

This is a search strategy for finding the local minimum of a function that can be differentiated, such as a loss function. Gradient descent algorithm (GDA) is mostly used in machine learning (ML) to determine the parameters/weights of a function that optimally reduces a cost function, algorithm steps as shown in (1) [20]. Repeat these steps until convergence is reached:

- Calculate the parametric changes as a function of the learning rate based on the gradient.
- Use the updated parameter value to recalculate the new gradient.
- Check for the termination criterion, else revert to step one.

The GDA is represented the θ parameter for optimization algorithm in the (1).

$$\theta_j \leftarrow -\alpha \frac{\partial}{\partial \theta_j} J(\theta) \quad (1)$$

As a configurable parameter, the learning rate has a small positive value ranging from 0.0 to 1.0; it is used to train neuron networks (NNs) (note that logistic regression is a NN with just one neuron) [21], [22]. Hence, the learning rate determines the rate of adaptation of the model to the situation. Some modifications in gradient descent algorithm and making workable for powerful deep neural networks [23], [24]. There are a few drawbacks of GDA, especially the required number of computations for each iteration of the algorithm. For instance, assume a case of 20,000 data points with 20 features; here, the sum of squared residuals will contain the same number of terms as the data points (that is 20,000 terms in this case). Hence, the derivative of this function must be computed based on each of the features. This will require the following computation: $20,000 \times 20 = 400,000$ computations in each iteration. If we consider 1,000 iterations, we may be arriving at $400,000 \times 1,000 = 400,000,000$ computations to fully implement the GDA which is much an overhead; hence, GDA is not usually fast on huge datasets, leading to the development of stochastic gradient descent (SGD). The term “stochastic” here means “random” which comes to play when data points are being selected at each step for the calculation of the derivatives. The SGD picks one data point randomly from the entire dataset per iteration to minimize the computation requirements [25].

In stochastic gradient descent, we are feeding only one data point at each iteration, but it is a very slow process so to make it speed we have to create batches like in each batch consists of 16, 32, 48, 64 data samples and training on batches make the training process fast and reduce the computation as well [26]–[28]. The Adam optimizer employs a hybrid of two gradient descent techniques: Momentum: This approach is used to speed up the GDA in consideration of the 'exponentially weighted average' of the gradients. The algorithm tends to converge rapidly towards the minima because it uses the averages. Root mean squared propagation (RMSprop) was proposed by Geoffrey Hinton as a gradient-based NN training approach. The gradients of complex functions, such as NNs tend to either vanish or explode as the data propagates through such function. RMS prop was created as a stochastic mini-batch learning algorithm that solves problems by normalizing the gradient with a moving average of squared gradients. This process of normalization equalizes the step size and either lower it for high gradients to prevent explosion or raise it for minor gradients to avoid vanishing. Simply expressed, RMSprop treats the learning rate as an adaptive parameter rather than a hyperparameter. This indicates that the rate of learning fluctuates with time.

2.5. Convolution layer

Convolutional layers are used to produce a larger receptive filter, which allows the model to recognize more input images features. Examining all of the pixels in an image is a simple way to process it; however, this can delay the training process dramatically. image pixels are sparse, there could be several zero pixels that

have no important feature of interest. So, convolution is the application of filter to an image and its subsequent swiping over to narrow down the underlying image to more specific and distinct features that are more specific to the considered object [29].

A “convolutional layer is made up of a series of filters, each of which has its own set of parameters that must be learned. The filter is slid over the input's width and height, and the dot products between the input and filter are calculated at each spatial position before being fed into an activation function. The convolutional layer's output volume is done by layering the activation maps of all filters along with the depth” dimension [30].

Image compression in the substituting the feature map output with a summary statistic of nearby outputs, the pooling layer compresses an image. For instance, the maximum statistic is used in max-pooling to decide a sliding window's result, leading to a down-sampled feature map with fewer redundant pixels and faster training and lower memory use. In average pooling, the sliding window's result is computed using the average statistic; so, the averaging of the feature map is first done before it is transferred to the next layer. Therefore, the use of the pooling layer when building a deep neural network (DNN) can significantly reduce the amount of information conveyed by an image [31].

This function is used mostly in problems that involve multiclass classification because of its desirable performance in real number value compression into a value range of [32] and ensuring that the sum of the whole probabilities of the output equals 1. It uses Sigmoid as an activation function to compress all input values into a value range between [32]. However, input values >0 produce a result >0.5 while those < 0 produces results <0.5 . Finally, any input with a 0 value produces a result equal to 0.5 [32]. Most times the sigmoid function is commonly used as the final output layer in binary classification problems [33].

The dropout process is a simple one; The addition of a dropout procedure after a neuron network layer either destroys or removes a random number of neurons. The chance of deleting a neuron is determined by the predefined dropout rate, p ; for instance, if $p= 0.5$, there is a 0.5 chance of losing every neuron before feeding to the next layer. The more the number of destroyed neurons, the greater the regularization impact. The downstream neurons' contribution to activation is temporally eliminated from the feed-forward path during the training phase, and their updated weight is not fed to the backward path neurons. Furthermore, the more the number of deleted neurons, the fewer the number of training samples for the subsequent layer, and this can cause the problem of underfitting. In practice, the hidden layer should have a typical dropout rate p in the range of 0.2 and 0.5, while that of the input layer is 0.2.

The training of DNNs is challenging for a variety of reasons, including the fact that the input from prior layers can change when weights are updated. Batch normalization is one of the network input standardization approaches that can be used for either prior layer activations or direct inputs. This process reduces generalization error by speeding up training and providing some regularization, in some cases halving epochs or more.

3. CONCLUSION

A model that fits well on the training data but performs poorly on unobserved data is said to be over-fitted. For instance, a 3-D function is used to fit a small dataset given by a 1-D function. In deep learning (DL), a model with much capacities, such as one that learns more function mapping from input to output, can learn too well and overfit the training dataset; this happens mostly when the function makes a prediction that fits too close to the data point. For this research, the first processing material needed is the unmanned aerial vehicle (UAV) remote sensing image; however, the acquired data from the camera sensor comes with several disadvantages. Hence, the first thing is to take some transportation before the labeling and training phase. Furthermore, CNN was used to process and extract road information from the UAV images. Owing to the huge number of parameters in the CNN, the result cannot be assured if the model is applied to actual road detection these parameters have been randomly initialized. As a result, the network parameters must be trained before using CNN in the real world. The initial stage in evaluating the effect of network training is to train and test the samples manually. The application area of CNN is limited by the enormous number of samples it requires. In this paper, manual sample data labeling fell well short of the number of samples required for network training. Studies have previously proved the efficacy of data augmentation in the training of network models. As a result, samples for network training were added based on the real scene via data augmentation.

ACKNOWLEDGEMENTS

The authors would like to acknowledge the financial support in the form of publication incentive grant from Universiti Malaysia Perlis (UniMAP).

REFERENCES

- [1] J. G. A. Barbedo, L. V. Koenigkan, T. T. Santos, and P. M. Santos, "A study on the detection of cattle in UAV images using deep learning," *Sensors*, vol. 19, no. 24, pp. 1–14, Dec. 2019, doi: 10.3390/s19245436.
- [2] M. A. Jishan, K. R. Mahmud, A. K. Al Azad, M. R. A. Rashid, B. Paul, and M. S. Alam, "Bangla language textual image description by hybrid neural network model," *Indonesian Journal of Electrical Engineering and Computer Science*, vol. 21, no. 2, pp. 757–767, Feb. 2021, doi: 10.11591/ijeecs.v21.i2.pp757-767.
- [3] B. Benjdira, Y. Bazi, A. Koubaa, and K. Ouni, "Unsupervised domain adaptation using generative adversarial networks for semantic segmentation of aerial images," *Remote Sensing*, vol. 11, no. 11, p. 1369, Jun. 2019, doi: 10.3390/rs11111369.
- [4] Aparna, Y. Bhatia, R. Rai, V. Gupta, N. Aggarwal, and A. Akula, "Convolutional neural networks based potholes detection using thermal imaging," *Journal of King Saud University - Computer and Information Sciences*, vol. 34, no. 3, pp. 578–588, Mar. 2022, doi: 10.1016/j.jksuci.2019.02.004.
- [5] S. Bhowmick, S. Nagarajaiah, and A. Veeraraghavan, "Vision and deep learning-based algorithms to detect and quantify cracks on concrete surfaces from UAV videos," *Sensors*, vol. 20, no. 21, pp. 1–19, Nov. 2020, doi: 10.3390/s20216299.
- [6] N. R. Shenoy and A. Jatti, "Ultrasound image segmentation through deep learning based improvised U-Net," *Indonesian Journal of Electrical Engineering and Computer Science*, vol. 21, no. 3, pp. 1424–1434, Mar. 2021, doi: 10.11591/ijeecs.v21.i3.pp1424-1434.
- [7] P. E. Carbonneau *et al.*, "Adopting deep learning methods for airborne RGB fluvial scene classification," *Remote Sensing of Environment*, vol. 251, p. 112107, Dec. 2020, doi: 10.1016/j.rse.2020.112107.
- [8] R. F. Olanrewaju, S. N. Ibrahim, A. L. Asnawi, and H. Altaf, "Classification of ECG signals for detection of arrhythmia and congestive heart failure based on continuous wavelet transform and deep neural networks," *Indonesian Journal of Electrical Engineering and Computer Science*, vol. 22, no. 3, pp. 1520–1528, Jun. 2021, doi: 10.11591/ijeecs.v22.i3.pp1520-1528.
- [9] N. Carion, F. Massa, G. Synnaeve, N. Usunier, A. Kirillov, and S. Zagoruyko, "End-to-end object detection with transformers," in *Computer Vision (ECCV) 2020*, Springer International Publishing, 2020, pp. 213–229.
- [10] S. Tongbram, B. A. Shimray, and L. S. Singh, "Segmentation of image based on k-means and modified subtractive clustering," *Indonesian Journal of Electrical Engineering and Computer Science*, vol. 22, no. 3, pp. 1396–1403, Jun. 2021, doi: 10.11591/ijeecs.v22.i3.pp1396-1403.
- [11] Q. Feng *et al.*, "Multi-temporal unmanned aerial vehicle remote sensing for vegetable mapping using an attention-based recurrent convolutional neural network," *Remote Sensing*, vol. 12, no. 10, p. 1668, May 2020, doi: 10.3390/rs12101668.
- [12] N. Horning, E. Fleishman, P. J. Ersts, F. A. Fogarty, and M. W. Zillig, "Mapping of land cover with open-source software and ultra-high-resolution imagery acquired with unmanned aerial vehicles," *Remote Sensing in Ecology and Conservation*, vol. 6, no. 4, pp. 487–497, Jan. 2020, doi: 10.1002/rse2.144.
- [13] M. S. AL-Huseiny and A. S. Sajit, "Transfer learning with GoogLeNet for detection of lung cancer," *Indonesian Journal of Electrical Engineering and Computer Science*, vol. 22, no. 2, pp. 1078–1086, May 2021, doi: 10.11591/ijeecs.v22.i2.pp1078-1086.
- [14] M. D. Hossain and D. Chen, "Segmentation for object-based image analysis (OBIA): a review of algorithms and challenges from remote sensing perspective," *(ISPRS) Journal of Photogrammetry and Remote Sensing*, vol. 150, pp. 115–134, Apr. 2019, doi: 10.1016/j.isprsjrs.2019.02.009.
- [15] M. Hossain and M. N. Sulaiman, "A Review on Evaluation Metrics for Data Classification Evaluations," *International Journal of Data Mining & Knowledge Management Process*, vol. 5, no. 2, pp. 01–11, Mar. 2015, doi: 10.5121/ijdkp.2015.5201.
- [16] K. Kim and H. S. Lee, "Probabilistic anchor assignment with IoU prediction for object detection," in *Computer Vision (ECCV) 2020*, vol. 12370, Springer International Publishing, 2020, pp. 355–371.
- [17] N. D. Al-Shakarchy and I. H. Ali, "Detecting abnormal movement of driver's head based on spatial-temporal features of video using deep neural network DNN," *Indonesian Journal of Electrical Engineering and Computer Science*, vol. 19, no. 1, pp. 344–352, Jul. 2020, doi: 10.11591/ijeecs.v19.i1.pp344-352.
- [18] N. Zheng, G. Loizou, X. Jiang, X. Lan, and X. Li, "Preface: computer vision and pattern recognition," *International Journal of Computer Mathematics*, vol. 84, no. 9, pp. 1265–1266, Sep. 2007, doi: 10.1080/00207160701303912.
- [19] A. Kirillov, Y. Wu, K. He, and R. Girshick, "Pointrend: image segmentation as rendering," in *2020 IEEE/CVF Conference on Computer Vision and Pattern Recognition (CVPR)*, Jun. 2020, pp. 9796–9805, doi: 10.1109/cvpr42600.2020.00982.
- [20] T.-Y. Lin, P. Dollár, R. Girshick, K. He, B. Hariharan, and S. Belongie, "Feature pyramid networks for object detection," in *2019 IEEE Conference on Computer Vision and Pattern Recognition (CVPR)*, Jul. 2019, pp. 428–431, doi: 10.1109/cvpr.2017.106.
- [21] S. Liu, L. Qi, H. Qin, J. Shi, and J. Jia, "PANet: path aggregation network for instance segmentation," in *2018 IEEE/CVF Conference on Computer Vision and Pattern Recognition*, Jun. 2019, pp. 8759–8768, doi: 10.1109/cvpr.2018.00913.
- [22] R. I. Farhan, A. T. Maolood, and N. F. Hassan, "Performance analysis of flow-based attacks detection on CSE-CIC-IDS2018 dataset using deep learning," *Indonesian Journal of Electrical Engineering and Computer Science*, vol. 20, no. 3, pp. 1413–1418, Dec. 2020, doi: 10.11591/ijeecs.v20.i3.pp1413-1418.
- [23] J. Pang, K. Chen, J. Shi, H. Feng, W. Ouyang, and D. Lin, "Libra R-CNN: towards balanced learning for object detection," in *2019 IEEE/CVF Conference on Computer Vision and Pattern Recognition (CVPR)*, Jun. 2019, pp. 821–830, doi: 10.1109/cvpr.2019.00091.
- [24] M. E. Paoletti, J. M. Haut, J. Plaza, and A. Plaza, "Deep learning classifiers for hyperspectral imaging: a review," *ISPRS Journal of Photogrammetry and Remote Sensing*, vol. 158, pp. 279–317, Dec. 2019, doi: 10.1016/j.isprsjrs.2019.09.006.
- [25] D. H. Jung, A. Sharma, and J. P. Jung, "A review of soft errors and the low $\alpha\beta$ -solder bumping process in 3-D packaging technology," *Journal of Materials Science*, vol. 53, no. 1, pp. 47–65, Jul. 2017, doi: 10.1007/s10853-017-1421-y.
- [26] S. Park and A. Song, "Discrepancy analysis for detecting candidate parcels requiring update of land category in cadastral map using hyperspectral UAV images: a case study in Jeonju, South Korea," *Remote Sensing*, vol. 12, no. 3, p. 354, Jan. 2020, doi: 10.3390/rs12030354.
- [27] G. Tsagkatakis, A. Aidini, K. Fotiadou, M. Giannopoulos, A. Pentari, and P. Tsakalides, "Survey of deep-learning approaches for remote sensing observation enhancement," *Sensors*, vol. 19, no. 18, pp. 1–39, Sep. 2019, doi: 10.3390/s19183929.
- [28] D. Tuija, C. Persello, and L. Bruzzone, "Domain Adaptation for the Classification of Remote Sensing Data: An Overview of Recent Advances," *IEEE Geoscience and Remote Sensing Magazine*, vol. 4, no. 2, pp. 41–57, Jun. 2016, doi: 10.1109/MGRS.2016.2548504.
- [29] A. S. Ahmed, H. M. Khudhur, and M. S. Najmuldeen, "A new parameter in three-term conjugate gradient algorithms for unconstrained optimization," *Indonesian Journal of Electrical Engineering and Computer Science*, vol. 23, no. 1, pp. 338–344, Jul. 2021, doi: 10.11591/ijeecs.v23.i1.pp338-344.
- [30] R. Vaddi and P. Manoharan, "CNN based hyperspectral image classification using unsupervised band selection and structure-preserving spatial features," *Infrared Physics & Technology*, vol. 110, p. 103457, Nov. 2020, doi: 10.1016/j.infrared.2020.103457.

- [31] F. N. Jardow and G. M. Al-Naemi, "A new hybrid conjugate gradient algorithm for unconstrained optimization with inexact line search," *Indonesian Journal of Electrical Engineering and Computer Science*, vol. 20, no. 2, p. 939, Nov. 2020, doi: 10.11591/ijeecs.v20.i2.pp939-947.
- [32] H. Zhang, H. Chang, B. Ma, N. Wang, and X. Chen, "Dynamic R-CNN: towards high quality object detection via dynamic training," in *Computer Vision (ECCV) 2020*, Springer International Publishing, 2020, pp. 260–275.
- [33] H. Zhang, M. Liptrott, N. Bessis, and J. Cheng, "Real-time traffic analysis using deep learning techniques and UAV based video," Sep. 2019, doi: 10.1109/avss.2019.8909879.

BIOGRAPHIES OF AUTHORS



Shouket Abdulrahman Ahmed    is awarded M.Sc. in Electrical System engineering, University Malaysia Perlis (UniMAP), Perlis, Malaysia, (2016), thesis title is "Electrical Intelligence System Based on Microcontroller for Power Station". Currently, His expertise is in the areas of power electronics. He has published more than three journal articles and conferences. After that, he obtained a Bachelor's degree (full time), in electrical and electronics Engineering, Grad 3 from Thames Polytechnic, UK (1989). He can be contacted at email: shouketunimap@gmail.com.



Hazry Desa    received his Bachelor of Mechanical Engineering from Tokushima University, Japan. He was a Senior Design Mechanical Engineer in R&D Sony Technology Malaysia in 1997. In 2001 he was employed by Tamura Electronics Malaysia. He pursued his PhD at the Artificial Life and Robotics Laboratory, Oita University, Japan in 2003. He has supervised a number of postgraduate students in either Master or Doctor of Philosophy levels. His research interests include mobile robot, unmanned systems and aerial robotics. A lot of achievements have been made through the years such as journal publications, patents and prototypes developments in UAS area. He is also registered with Engineering Council United Kingdom as Chartered Engineer (CEng), registered as a Professional Engineer (Ir.) with Board of Engineers Malaysia (BEM), registered as a Professional Technologist (Ts.) with Malaysia Board of Technologist (MBOT), senior member of IEEE and a member of IET. He can be contacted at email: hazry@unimap.edu.my.



Abadal-Salam T. Hussain    is currently a PhD faculty staff, Assistant Professor-Department head of Medical Instrumentations Technique Engineering, Al-Kitab University. Previously Faculty staff of School of Electrical System Engineering, University Malaysia Perlis (UniMAP), Malaysia (2013-2016). Before that, he was affiliated with the University of Sharjah, UAE (2004-2007) and "Sharjah Institute of Technology (SIT), Sharjah, UAE (2007-2011). Abadal also has a GCE from the University of London & a Bachelor of Engineering from the Royal Naval Engineering College, Manadon, Plymouth, UK in (1989). He also has a Master of Science awarded by the University of Science & Technology Oran Algeria in 2000 and a doctorate (PhD) in Mechatronic Engineering awarded by the University Malaysia Perlis (UniMAP) in 2013. He can be contacted at email: asth2233@gmail.com, asth3@yahoo.com.